Biophysical Chemistry, 38 (1990) 241–263
Elsevier

BIOCHE 01520

Kinetics and thermodynamics of metabolite transfer between enzymes

Paul Smolen and Joel Keizer

Biophysics Graduate Group, Department of Chemistry, and Institute of Theoretical Dynamics, University of California, Davis, CA 95616-8618, U.S.A.

Received 30 March 1990
Revised manuscript received 21 June 1990
Accepted 21 June 1990

Metabolic channeling; Direct transfer; Enzyme-enzyme interaction

Based on experimental evidence put forward by Bernhard and others, we explore the kinetics and thermodynamics of the proposed direct and diffusional transfer mechanisms of enzymatic catalysis. Data for transient transfer of NADH between two cognate dehydrogenases (E1 and E2) are combined with steady-state catalytic data to quantify the kinetics of the two transfer mechanisms. In order to rationalize these data we find: (1) that the rate constants for direct transfer of NADH from E1-NADH to E2 must be much larger when a reactive metabolite, M, is bound to E2, (2) that a significant amount of noncatalytic complex E1–E2-M must be formed, and (3) that dissociation constants of the order of 1 μM are required for the ternary complexes involved in direct transfer (E1-NADH-E2). Using values of rate parameters similar to those assumed in these calculations, we proceed to explore the kinetics and thermodynamics of a hypothetical two-enzyme segment of a metabolic pathway that involves direct and diffusional metabolite transfer operating in parallel. Under steady-state conditions, we conclude from our calculations: (1) that the flux through the direct transfer branch would be comparable to or greater than that through the diffusional transfer branch under physiological conditions, (2) that activity effects resulting from physiological concentrations of inert protein enhance the predominance of the direct transfer flux, (3) that significant concentrations of ternary transfer complexes are formed, (4) that changes in the catalytic mechanism involving the ternary complex have little effect, (5) that direct transfer significantly moderates the reduction in metabolic flux caused by protein complexation, and (6) that direct transfer greatly alters the thermodynamics and kinetics of our hypothetical pathways. We conclude, therefore, that direct transfer — when it exists — would have important kinetic, thermodynamic, and physiological consequences in vivo.

1. Introduction

In recent years it has become increasingly clear [1,2] that metabolism as it occurs in vivo is more than merely a sequence of the component catalytic reactions that have been characterized in vitro using dilute, purified enzymes [3]. Indeed, the concentrations of the glycolytic enzymes in muscle sarcoplasmic fluid are comparable to or exceed those of the glycolytic intermediates [4]. This implies that intermediates, which are predominantly free in solution when enzymes are present in catalytic amounts in vitro, may well be predominantly bound in vivo. Furthermore, the high concentration of protein in the cytoplasm of cells implies that activity effects, not relevant in dilute solution, may be significant. The existence of structural elements with the cytoplasm, including the endoplasmic reticulum, microtubules, and other cytoskeletal elements, provides the opportunity for immobilization and clustering of enzymes [5]. Indeed, in the concentrated environment of the cytoplasm many complex protein-protein interactions that could affect individual or neighboring steps in a metabolic pathway seem possible.

Correspondence address: J. Keizer, Institute of Theoretical Dynamics, University of California, Davis, CA 95616-8618, U.S.A.

At the present time, little is known about the consequences for metabolism of the complex physico-chemical conditions that exist in the cytoplasm. One of the mechanisms that have been proposed to operate in this milieu is 'channelling', in which metabolites are supposedly passed directly from one enzyme to another [6,7]. One form of channelling, called 'direct transfer', recently has been studied in some molecular detail for the glycolytic enzymes. This mechanism involves the formation of transient 'ternary complexes' between two enzymes that share a common metabolite and the metabolite itself. The evidence for these complexes is based on kinetic experiments with concentrated enzyme solutions in vitro [8–10]. According to these experiments, the complexes are distributed homogeneously in solution and are competent to transfer the common metabolite directly from one active site to the other, without equilibration of the intermediate with the surrounding solution during the transfer process. Bernhard [4,11] referred to this process as the direct transfer mechanism, while the corresponding process in which the common metabolite is released by one enzyme into solution before being bound to the second is termed 'diffusional transfer'.

The phenomenon of direct transfer has been invoked to explain the steady-state kinetics for the glycolytic enzymes lactate dehydrogenase (LDH), glyceraldehyde phosphate dehydrogenase (GPDH), and phosphoglycerate kinase (PGK), among others. Srivastava and Bernhard have presented further evidence that LDH and GPDH transfer reduced nicotinamide adenine dinucleotide (NADH) directly [9], and using stopped-flow kinetic techniques have suggested that transfer takes place as a unimolecular process within a ternary complex [10,12,13]. Some of the findings of direct transfer, however, are controversial. Indeed, while Weber and Bernhard [8] report evidence that PGK and GPDH transfer 1,3-diphosphoglycerate (DPG) directly, Kvassman and Pettersson [14,15] recently have found fault with Weber and Bernhard's interpretation of their data as well as the suggestion that direct transfer occurs between aldolase and GPDH [16]. On the other hand, the observation that dehydrogenases of differing stereospecificity ('A' vs 'B') exhibit direct transfer of NADH according to the enzyme buffering criterion of Bernhard and Srivistava [9,11], while pairs of like stereospecificity (A, A or B, B) do not, seems like compelling evidence in favor of the direct transfer mechanism. This observation is reinforced by molecular modelling of the NADH binding sites and the way that the dehydrogenases of differing stereospecificity can fit together [17]. Yet, the invocation of direct transfer to explain the kinetics of pairs of dehydrogenases at high concentration also has its critics. Recently, Chock and Gutfreund [18] have asserted that diffusional transfer alone suffices to explain both the transient and steady-state kinetics of NADH transfer between the A-B pair of α-glycerol-3-phosphate dehydrogenase (GDH) and LDH. Nonetheless, a reinvestigation of this pair by several different research groups appears to have refuted this challenge [12].

In an effort to help sort out this controversy, as well as to clarify the implications of these two transfer mechanisms, we have conducted a theoretical investigation of the kinetics and thermodynamics of both direct and diffusional transfer between pairs of enzymes. The mechanistic complexity of such systems is a strong justification for a theoretical approach to this problem. Indeed, direct transfer involves a kinetic coupling within a cognate enzyme pair (e.g., A and B dehydrogenases) and, thus, dramatically increases the number of intermediates involved in the transfer process, e.g., free metabolites and their enzymes and their binary and ternary complexes. Direct and diffusional transfer operate as parallel, competitive mechanisms, although diffusional transfer is obviously overwhelmingly favored when enzyme concentrations are low. Thus, the effect of varying enzyme concentrations must be investigated. In addition, using appropriate kinetic schemes, theoretical calculations can be employed to answer questions that are difficult to attack experimentally. In particular, it is easy in these calculations to vary rate constants, activities, enzyme concentrations, etc., in order to determine conditions under which one or the other transfer mechanism dominates. Using the modern theory of irreversible processes [19], which contains both the kinetic

and thermodynamic aspects of molecular mechanisms, it is further possible to examine the consequences of direct transfer for the thermodynamics of intermediary metabolites.

In order to carry out such calculations it is necessary to have realistic values for kinetic parameters. Fortunately, sufficient data are available from the transient and steady-state experiments described above to estimate most of the parameters required for the kinetic analysis. In order to make these estimates, we have carried out an analysis of the NADH-dehydrogenase data. This demonstrates another value of our theoretical approach, namely, to estimate parameters that have been difficult to measure experimentally, such as association and dissociation constants for ternary complexes, by choosing them to fit experimentally measured kinetic data. Assuming simple kinetic schemes which include both direct and diffusional transfer steps in competition, we have been able to rationalize simultaneously both the stopped-flow and steady-state data for A-B dehydrogenase pairs. In order to do so, however, we have needed to make additional mechanistic assumptions which, nonetheless, should be easy to test experimentally.

To develop qualitative information about the importance of the direct transfer mechanism, relative to diffusional transfer, in vivo, we have explored the kinetics and thermodynamics of several hypothetical two-enzyme 'pathways'. These pathways involve the catalytic conversion of an initial metabolite, M1, to a final metabolite, M3, via an intermediate metabolite, M2. M2 is a product of the first enzyme, E1, and a reactant for the second, E2. The pathways permit transfer of M2 between the enzymes by either the direct or diffusional mechanisms. Since the mechanisms are competitive, we were able to assess the range of rate constants and enzyme concentrations for which direct transfer contributes significantly to the flux through a pathway. We found that, under physiological conditions of enzyme concentrations and rate constants, the steady-state flux through the direct transfer branch is comparable to or exceeds that through the diffusional transfer branch when the concentration of E2 exceeds E1 and the association rate constant for E1-M2 with E2 is greater than 10^7 M^{-1} s^{-1}. Examining three variants of this pathway, we also found that changing the details of the mechanism, for example, whether or not catalysis occurs within the ternary complex, does not change this conclusion. If noncatalytic binary complexes can form between the two enzymes, the existence of direct transfer strongly moderates the decrease in flux associated with the formation of the inactive complex. We also examined the effect of activity coefficients on the kinetics of these pathways using a simple implementation of scaled particle theory [20] for estimation of these coefficients. Our calculations demonstrate that activity effects, which result from adding to the model inert protein present at a high concentration similar to that found in vivo, greatly enhance the efficacy of the direct transfer mechanism.

In order to determine to what extent the direct transfer mechanism might modify the thermodynamics of a pathway, we calculated Gibbs free energy differences and the rate of dissipation of free energy for the steps in the pathway. Here, again, we found that when direct transfer is competitive with diffusional transfer these quantities can be modified significantly. In particular, the rate of dissipation of free energy in steps involving association of enzymes to form ternary complexes can be quite high. Finally, we examined the distribution of metabolites among ternary complexes, binary enzyme-substrate complexes, and solution, and the manner in which this is affected by alterations in activity coefficients and in the dissociation equilibrium constants for ternary and noncatalytic enzyme complexes.

2. Theoretical background

To study the kinetics and thermodynamics of a pathway, it is necessary to construct a system of differential equations that describes the time evolution of the concentrations of the relevant species. In order to do this we have relied on the modern theory of nonequilibrium thermodynamics, which is applicable to systems that are far from equilibrium [19]. To apply this theory, one begins by identifying the elementary molecular

processes in the mechanism of interest. For a metabolic pathway, the elementary processes are individual binding or catalytic steps, each characterized by a forward and reverse rate constant. Two examples are the bimolecular association of enzyme and substrate to form an enzyme-substrate complex

$$\mathrm{E} + \mathrm{S} \underset{k_{-1}}{\overset{k_{+1}}{\rightleftharpoons}} \mathrm{E\text{-}S} \tag{1}$$

and the unimolecular conversion of one enzyme-substrate complex into another, either via catalysis or by the direct transfer of an intermediate within an enzyme-enzyme complex

$$\mathrm{E\text{-}S1} \underset{k_{-1}}{\overset{k_{+1}}{\rightleftharpoons}} \mathrm{E\text{-}S2}. \tag{2}$$

There is a general, thermodynamic formula for the rate of these or any other elementary processes [19]. Defining the local equilibrium chemical potential in the usual way by

$$\mu_i = \mu_i^0 + \mathrm{RT} \ln a_i$$

where a_i is the thermodynamic activity of species i, the net rate, R_1, of the association process in eq. 1 can be written in canonical form as

$$R_1 = \Omega_1 \left\{ \exp\left[\frac{(\mu_S + \mu_E)}{RT} \right] - \exp\left[\frac{\mu_{ES}}{RT} \right] \right\} \tag{3}$$

where Ω_1 is called the 'intrinsic rate' of the elementary process. In the usual concentration units, R_1 is the rate in mol l^{-1} s^{-1} of the association reaction, with the direction of association taken as positive. Similarly, for the catalytic process in eq. 2, we have

$$R_2 = \Omega_2 \left\{ \exp\left[\frac{(\mu_{E-S1})}{RT} \right] - \exp\left[\frac{\mu_{E-S2}}{RT} \right] \right\} \tag{4}$$

with Ω_2 its intrinsic rate.

If we substitute the definition of the local equilibrium chemical potential into the expression in eq. 3 for the net rate of the first process, we find that

$$R_1 = k_{+1} a_E a_S - k_{-1} a_{E\text{-}S} \tag{5a}$$

where

$$k_{+1} = \Omega_1 \exp\left[\frac{(\mu_S^0 + \mu_E^0)}{RT} \right]$$

and

$$k_{-1} = \Omega_1 \exp\left[\frac{\mu_{E\text{-}S}^0}{RT} \right]$$

are rate constants depending only on the temperature.

For the catalytic process the rate of which is given in eq. 4, we may readily write down an equation analogous to eq. 5a,

$$R_2 = k_{+1} a_{E\text{-}S1} - k_{-1} a_{E\text{-}S2} \tag{5b}$$

If we now replace the activity of species i, a_i, by the concentration of species i, which we denote as [i], via the usual thermodynamic relation $a_i = \gamma_i[\mathrm{i}]$ (γ_i, activity coefficient), we obtain from eq. 5a the result

$$R_1 = k_{+1} \gamma_E \gamma_S [\mathrm{E}][\mathrm{S}] - k_{-1} \gamma_{ES} [\mathrm{E\text{-}S}] \tag{6}$$

In dilute solution where the activity coefficients are all unity, eq. 6 becomes the familiar expression for the rate of association given by the mass-action law, while in concentrated solution it provides the usual activity correction to the rate.

In formulating the systems of differential equations for our pathways, we made systematic use of the canonical form, applying it to each elementary process. Thus, for the association of enzyme and substrate we have

$$R_1 = \frac{\mathrm{d}[\mathrm{E\text{-}S}]}{\mathrm{d}t} = k_{+1} \gamma_E \gamma_S [\mathrm{E}][\mathrm{S}] - k_{-1} \gamma_{ES} [\mathrm{E\text{-}S}]. \tag{7}$$

and from eq. 5b we obtain

$$R_2 = \frac{\mathrm{d}[\mathrm{E\text{-}S2}]}{\mathrm{d}t} = -k_{-1} \gamma_{ES2} [\mathrm{E\text{-}S2}] + k_{+1} \gamma_{ES1} [\mathrm{E\text{-}S1}] \tag{8}$$

The systems of differential equations corresponding to all the mechanisms that we have dealt with can be integrated accurately with standard numerical techniques. For this we have used the

ordinary differential equation solver PLOD [21], which is based on the Gear algorithm [22].

The local equilibrium chemical potentials can be used to define the change in free energy per unit of increase in the extent of reaction for an elementary process. The following process contains as special cases all the processes we shall deal with.

$$\upsilon_a A + \upsilon_b B \underset{k_{-1}}{\overset{k_{+1}}{\rightleftharpoons}} \upsilon_c C + \upsilon_d D. \tag{9}$$

Here υ_i denotes the stoichiometric coefficient of species i. The extent of reaction increases by one when υ_a moles of A and υ_b moles of B are consumed, producing υ_c moles of C and υ_d moles of D. The change in Gibbs free energy is then given by $\Delta G = \upsilon_c\mu_c + \upsilon_d\mu_d - \upsilon_a\mu_a - \upsilon_b\mu_b$ [23], and if we again substitute $\mu_i = \mu_i^0 + \mathrm{RT}\ \ln\ a_i$ we obtain the usual expression

$$\Delta G = \Delta G^0 + RT\ \ln\ Q \tag{10}$$

with

$$\Delta G^0 = -RT\ \ln\left\{\frac{k_{+1}}{k_{-1}}\right\} = -RT\ \ln\ K_{eq} \tag{11a}$$

and

$$Q = \left(\frac{a_c^{\upsilon_c} a_d^{\upsilon_d}}{a_a^{\upsilon_a} a_b^{\upsilon_b}}\right). \tag{11b}$$

The quantity ΔG^0 is the Gibbs free energy change for reactants and products in their standard states and is related to the equilibrium constant, K_{eq}, as in eq. 11a. The rate of dissipation of free energy by an elementary process i, Φ_i, is then given by the rate of that elementary process multiplied by the change in free energy for that elementary process, i.e.

$$\Phi_i = R_i \Delta G_i. \tag{12}$$

Another derivation of eq. 12 can be found in ref. 24.

For our simulations we required a method to assign plausible values to the activity coefficients of protein species. An approximate theory for proteins, based on scaled-particle theory, has been developed by Minton and Ross [25]. This theory approximates each protein species by a species of hard particle, most commonly a sphere of a certain radius, and then calculates activity coefficients for each species by use of an equation developed by Ross and Minton [26]. This equation is given in the appendix to the present paper (eq. A1). This theory takes into account electrostatic effects somewhat crudely by allowing for an 'effective radius' of the hard sphere larger than the radius of the protein as determined by physical measurements. The theory has accounted quantitatively for light scattering of bovine serum albumin (BSA) solutions as concentrated as 90 g/l [27], and for osmotic pressure and sedimentation equilibria in solutions of hemoglobin as concentrated as 350 g/l [28]. It has also predicted semiquantitatively the dependence of the catalytic rate of GPDH on the concentration of inert protein [29]. Thus, we have used this theory to calculate activity coefficients for the protein species in our mechanisms, bearing in mind that the 'physiological' concentration of protein in cells is in the range of 200–400 g/l [4], a range which our simulations reflect.

3. Direct transfer of NADH among dehydrogenases

Direct transfer of NADH among dehydrogenases has been established primarily via a steady-state 'enzyme buffering' technique pioneered by Weber and Bernhard [8]. In this technique, the concentration of free metabolite, M1, is driven to a very low level by combination with an enzyme, E1. A second enzyme, E2, which requires M1 for its catalytic step, is then introduced and the velocity of the E2-catalyzed reaction with this metabolite is measured. A velocity in excess of that which can be accounted for by the concentration of free metabolite indicates that the complex E1-M1 is itself combining with the second enzyme, with transfer of the metabolite to E2 occurring when this ternary complex is formed. The essential steps in the direct transfer mechanism are thus

$$\begin{aligned}\text{E1-M} + \text{E2} &\rightleftharpoons \text{E1-M---E2} \rightleftharpoons \text{E1---M-E2} \\ &\rightleftharpoons \text{E1} + \text{M-E2}\end{aligned} \tag{13}$$

The enzyme buffering technique suggests [9] that when the concentration of E1-M is high enough this mechanism competes with the diffusional transfer mechanism,

$$\text{E1-M} \rightleftharpoons \text{E1} + \text{M}$$
$$\text{E2} + \text{M} \rightleftharpoons \text{E2-M}, \qquad (14)$$

which proceeds without the formation of ternary complex.

Transient kinetic experiments have also provided evidence for enzyme-enzyme interactions among A-B pairs of dehydrogenases. In this type of experiment a solution of NADH and E1, with the enzyme in excess so that most of the NADH is bound, is mixed in a stopped-flow apparatus with a solution containing E2 [10]. Because the fluorescence emission spectrum of bound NADH differs for each enzyme, one can follow the equilibration of NADH between the two enzymes in the solution. It has been found [10,12] that the time course of equilibration of the fluorescence can be fitted quite well by a single exponential, so that an approximate equilibration 'rate constant' can be determined. If the association and dissociation rate constants of NADH from the enzymes are known, then the course of this equilibration can also be simulated by numerical integration of the differential equations for the diffusional transfer mechanism [12,18] which gives a predicted rate constant. It has been found [12] for a range of enzyme concentrations that the observed rate constant for equilibration for the A-B pair LDH and GDH is slower by an approximate factor of two than the predicted rate based on the diffusional transfer mechanism. This argues for an interaction between the enzymes that alters the kinetics of the equilibration, and suggests that the rate constants for the steps in direct transfer of NADH are relatively small.

Experimental determination of the association and dissociation rate constants for ternary complex formation, or of the transfer rate constants for NADH within these complexes, has proven difficult. Thus, we determined to estimate these parameters by numerical simulation to fit the existing steady-state and transient data. Lacking mechanistic information, we have assumed the simplest possible mechanisms. The mechanism for simulation of the transient experiments, termed Scheme I, and that for simulation of the steady-state experiments, termed Scheme II, are both given in fig. 1. Both allow for diffusional as well as direct transfer of NADH from E1 to E2. Note that in Schemes I and II, and all schemes that follow, we have utilized a single line to represent the forward and reverse steps of a single elementary process. We have also adopted the usual convention that species connected by lines that join at an acute angle are simultaneously products (or reactants) of a given process. In Scheme II E2* represents E2 in the presence of its reactant metabolite (e.g., pyruvate if E2 is LDH), the arrow between E2-NADH and product represents an irreversible catalytic process with a rate given by a Michaelis-Menten expression with a Michaelis constant K_M and a catalytic rate constant k_{cat1}, and the arrow joining E1--NADH-E2 to product represents an irreversible catalytic step with a rate constant k_{cat2}.

Our initial simulations attempted to fit the steady-state and transient data obtained by

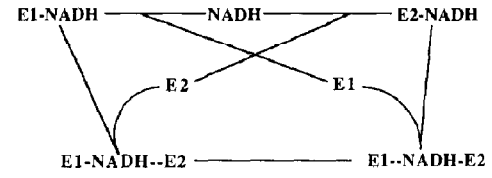

Scheme II

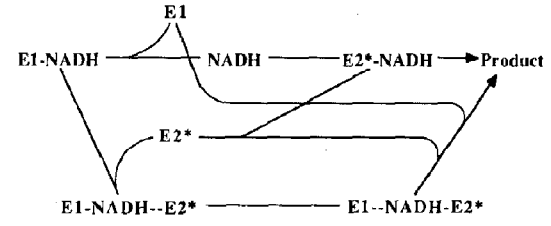

Fig. 1. (Top) The scheme used for simulations of the transient kinetic experiments with LDH and α-GDH [4,12] and (below) the scheme used for simulations of the corresponding steady-state kinetic experiments [9,12].

Srivastava and Bernhard for the most thoroughly investigated A-B pair, that of pig heart LDH and rabbit muscle α-GDH. We fixed the association and dissociation rate constants of free NADH from these enzymes, and the Michaelis constants and turnover numbers of these enzymes for free NADH, at the values listed in table 1, which have been determined experimentally [12]. For the association and dissociation processes associated with formation of the postulated ternary complexes in Scheme I and for the transfer of NADH within the complexes, we sought values of the rate constants that would yield simulations agreeing with the time course of stopped-flow experimental measurements. To simplify our calculations, we neglected the effect of changing concentrations on the activity coefficients in the rate equations for Scheme I (cf. eqs 7 and 8). Thus, the activity coefficients were assumed to be constant and their values absorbed into the definition of the rate constants. Our calculations were performed by integrating the rate equations numerically using PLOD and plotting, vs time, the logarithm of a quantity I proportional to the fluorescence intensity. Neglecting free NADH because of its low concentration, the fluorescence intensity is given by adding the concentrations of the enzyme species with bound NADH together, each multiplied by the weighting factor of its intrinsic fluorescence intensity at unit concentration. Srivastava and Bernhard [10] have determined that the intrinsic fluorescence intensity of α-GDH-NADH is very close to twice that of LDH-NADH if the excitation is at a wavelength of 340 nm and the emission is monitored at a wavelength of 460 nm. In the absence of other information, we have assumed, as did Srivastava and Bernhard [10], that the intrinsic fluorescence intensity of NADH bound to LDH remains unchanged if α-GDH is also bound to form the ternary complex LDH-NADH--GDH, and similarly for NADH bound to GDH. Thus

$$I = [\text{LDH-NADH}] + 2[\alpha\text{-GDH-NADH}] + [\text{LDH-NADH--GDH}] + 2[\text{LDH--NADH-GDH}]. \quad (15)$$

We note that the time course of the intensity of fluorescence calculated using eq. 15 is not sensitive to the precise relative values that are assumed for the intensity of the various species, with changes of 50% causing only minor changes in the calculated equilibration rate.

The equilibration rate constant was taken from the slope of the logarithmic plot. As a check on accuracy, representative plots of I itself vs time were curve-fitted by an exponential, and the rate constants obtained by the two methods were found to agree. Using plausible values of association, dissociation, and transfer rate constants for the ternary complexes we fitted the experimental equilibration rates in either direction (LDH-NADH to α-GDH and vice versa) as a function of the total concentration of E2. The experimental equilibration rate constants, those calculated via simulation, and the values from simulation for association, dissociation, and transfer rate constants for the ternary complexes, are presented in table 2. This table also contains, for comparison, the calculated equilibration rate constants if no ternary complexes were forming and diffusion alone was responsible for the transfer of NADH between the enzymes, determined by integration of the rate equations appropriate to this case. Note that the assumed direct transfer rate constant of 32 s^{-1} reduces the equilibration rates by about 50% from

Table 1

Values of kinetic parameters for the interaction of NADH with pig heart LDH and rabbit muscle α-GDH (from ref. 12)

	Dissociation rate constant (k_{-1}) (s^{-1})	Association [a] rate constant (k_{+1}) ($M^{-1}\,s^{-1}$)	Michaelis constant (μM)	Turnover number (s^{-1})
Pig heart LDH	95	1.86×10^8	7.1	82.8
Rabbit α-GDH	135	1.69×10^8	2.4	57.7

[a] Calculated from the measured dissociation constant, K_d, according to: $K_d = k_{-1}/k_{+1}$.

Table 2

Simulation of transient stopped-flow kinetic data for the transfer of NADH between LDH and α-GDH

Experimental data taken from ref. 12 and Srivastava and Smolen (unpublished results). In this table, and subsequently, μN refers to the concentration of active sites. For the simulation, LDH-NADH combines with GDH with an on-rate constant of 1.0×10^8 M^{-1} s^{-1} and an off-rate constant of 220 s^{-1}, GDH-NADH combines with LDH with the same on-rate constant and with an off-rate constant of 158 s^{-1}, and within the ternary complex NADH is transferred in both directions with the same rate constant of 32 s^{-1}.

LDH-NADH transferring to GDH, with 7.5 μN [LDH-NADH] and 2.5 μN [LDH] as initial mixed concentrations:

[GDH] (μN)	Observed equilibration rate constant (s^{-1})	Calculated equilibration rate constant (s^{-1})	Calculated rate constant (s^{-1}) with diffusion only
7.5	78	90	160
12.5	73	81	146
20	83	74	132
32.5	64	67	121
47.5	63	61	118

GDH-NADH transferring to LDH, with 7.5 μN GDH-NADH and 2.5 μN GDH as initial mixed concentrations:

[LDH] (μN)	Observed equilibration rate constant (s^{-1})	Calculated equilibration rate constant (s^{-1})	Calculated rate constant (s^{-1}) with diffusion only
7.5	112	115	216
12.5	80	90	180
20	78	77	160
32.5	61	67	151
47.5	64	61	146

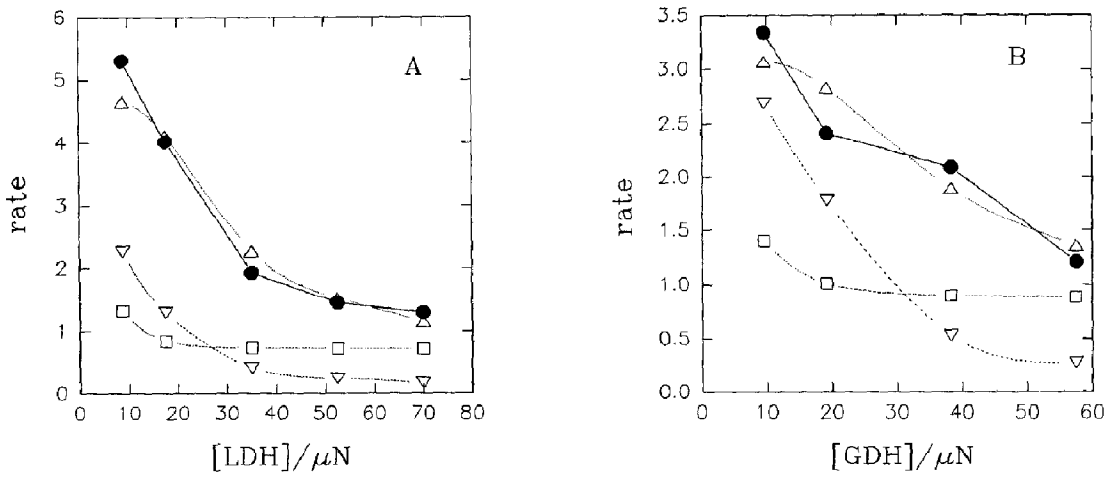

Fig. 2. (A) Analysis of the experimental steady-state kinetic data of Srivastava et al. [12] with the buffering enzyme, E1, being LDH, and the catalytic enzyme, E2, being GDH. (B) Analysis of analogous data with E1 being GDH and E2 LDH. The units for the rate of reaction are μM s^{-1}, and those for enzyme concentration are μN. (●) Experimental data; (▽) the rates expected if diffusion alone is responsible for the transfer of NADH from E1 to E2; (□) the rates expected if direct transfer and diffusion share responsibility for NADH transfer, assuming the values for association, dissociation, and transfer rate constants given in table 2; (△) the rates expected if direct transfer and diffusion share responsibility for NADH transfer with the following modification of the parameters in table 2: direct transfer rate constants increased to 700 s^{-1}; the k_{cat} for E1-NADH reacting with E2 increased to 400 s^{-1} when E2 is GDH and 150 s^{-1} when E2 is LDH; and with catalytically inactive E1-E2 complex forming with an association rate constant of 1.0×10^8 μM^{-1} s^{-1} and a dissociation rate constant of 185 s^{-1}.

the values given by diffusional transfer alone. This produces close agreement with the experimental values.

We analyzed steady-state experiments on this same pair of dehydrogenases via numerical integration of Scheme II. Lacking other information, we assumed the k_{cat} (turnover number) for E1-NADH reacting with E2* was the same as that for free NADH reacting with E2 (table 1). Our results for the steady-state rates vs [E1] are given in fig. 2 for E1 = GDH or LDH. Observed rates, given as filled circles, clearly cannot be reproduced by the rates, given as inverted triangles, predicted if only diffusional transfer of NADH occurs. Calculated rates using the association, dissociation, and transfer rate constants from table 2 that fit the transient kinetic data are given as squares. One notes that there is a sharp decrease in observed rates with increasing [E1], which is not reflected in the calculated rates. This argues that inhibition by excess E1 must be occurring, as previously suggested for this and other cognate dehydrogenase pairs [9]. Also, since the calculated rates are considerably lower than those observed, especially for low concentrations of E1, the transfer rate constants within the complex are apparently considerably higher under the conditions of the steady-state experiments than is the case for the stopped-flow experiments. It is possible that the second substrate required for oxidation of NADH by E2 (pyruvate for LDH and dihydroxyacetone phosphate for α-GDH) may interact with E2 to provide the necessary enhancement of this rate constant.

To determine the required magnitude of inhibition by excess E1 and enhancement of the direct transfer rate constants by the second substrate via further simulations, we added another step to Scheme II, namely,

$$\text{E1} + \text{E2}^* \underset{k_d}{\overset{k_a}{\rightleftharpoons}} \text{E1-E2}^*. \qquad (16)$$

It is implied here that the species E2* is significantly different from E2 and is thus able to bind to E1. In order to achieve agreement with experiment, there must exist strong interaction between E1 and E2*. Specifically, we assigned the forward and reverse rate constants for this step the values of $k_a = 1.0 \times 10^8$ M^{-1} s^{-1} and $k_d = 185$ s^{-1}, respectively. The k_{cat} for the reaction of E1-NADH with E2 also needed to be set somewhat higher than that for the reaction of free NADH with E2, to 400 s^{-1} if E2 is GDH and to 150 s^{-1} if E2 is LDH. Also, the rate constants for transfer of NADH within the complex both needed to be increased substantially, to 700 s^{-1}. With these modifications, we were able to reproduce the observed data rather closely. The data obtained are indicated by right-side-up triangles in fig. 2.

We are not entirely comfortable with the very low predicted inhibition constant for catalytically inactive complex formation, $K_i = k_d/k_a = 1.85$ μM, nor with the small values of the dissociation constants of 2.2 and 1.58 μM for the two ternary complexes. Indeed, we have investigated the amount of E2 found in ternary and inactive complexes under the conditions of fig. 2. It varies from 30 to 96% of the total E2 present. We have also investigated the amount of E2 found in ternary complexes under the conditions of table 2. It varies from 43 to 61% of the total E2 present, and would become considerably higher if the amount of NADH in the system was equal to or greater than that of E2, since an NADH is required for each complex. Such strong protein-protein interactions are absolutely required for explaining the data in a consistent manner. Previously, Srivastava and Bernhard estimated K_m values of 2.60 μM for halibut LDH-NADH as a substrate for halibut GPDH, 5.88 μM for halibut GPDH-NADH as a substrate for halibut LDH, and 1.21 μM for halibut LDH-NADH as a substrate for rabbit muscle GDH [9], so there is some precedent for strong protein-protein interactions in these systems. Also essential is a substantial enhancement of the rate constants for NADH transfer within the ternary complexes in the presence of the second substrate, and an enhanced rate of catalysis following this transfer step. Clearly, a more thorough experimental characterization of the putative ternary complexes is necessary before further calculations are justified.

Comparable calculations for other cognate dehydrogenase pairs exhibited a similar pattern when we attempted to reconcile the transient and steady-state kinetic experiments using Schemes I

and II. This suggests that strong protein-protein interactions and enhancement of the direct transfer of NADH in the presence of a second substrate may be common features of dehydrogenase reactions.

4. Hypothetical two-enzyme pathways

The kinetic data for dehydrogenases analyzed in section 3 are consistent with the idea that enzyme-enzyme complexes can participate in the direct transfer of metabolite. The mere existence of such a transfer mechanism, however, does not imply that it is important under physiological conditions. Indeed, the formation of an appreciable concentration of the ternary complexes that are required for direct transfer will occur only at high concentrations of the participating enzymes. Certainly in dilute enzyme solutions, typical of most in vitro experiments, diffusional transfer will dominate due to the low concentration of complexes. It is not at once obvious, however, whether diffusional transfer will continue to dominate direct transfer when enzyme concentrations reach the high levels encountered in vivo. In sarcoplasm, for example, the concentration of GPDH is 1.4 mM while that of LDH is 0.3 mM and that of enolase is 0.5 mM [4]. We have seen already in the preceding section that the presence of elevated concentrations (0.1 mM or greater) of LDH or α-GDH can reduce the transfer equilibration rate of NADH between these enzymes by a factor of two. Thus, it is plausible that at physiological concentrations direct transfer can compete effectively in catalytic pathways with diffusional transfer.

To investigate this question more quantitatively, we have examined the kinetic and thermodynamic properties of four short, hypothetical enzyme pathways that convert an initial metabolite, M1, to a product metabolite, M3. Each of these pathways involves two enzymes, E1 and E2, and is a variant of pathway A, which is shown in fig. 3 with the steps numbered for reference. Pathway A involves the conversion of M1 to an intermediate metabolite, M2, which is the catalytic product for E1 and a catalytic reactant for E2, while M3 is the

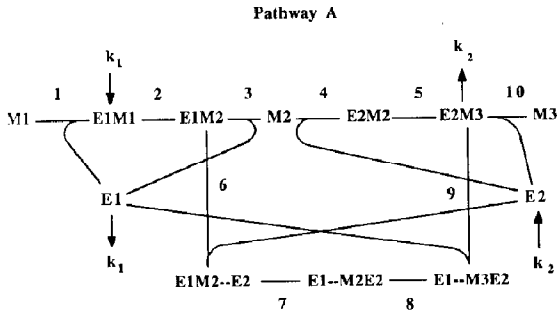

Fig. 3. The hypothetical two-enzyme pathway A. The parameters k_1 and k_2 are the input and output rate constants, termed k_{in} and k_{out} in the text. The individual elementary processes are numbered for reference.

product of the E2 catalyzed reaction. In this pathway the transfer of M2 from E1 to E2 can occur either by diffusional transfer (steps 3 and 4) or by direct transfer (steps 6 and 7). In order to obtain information about the relative efficiencies of the two transfer mechanisms, we have added input and output terms indicated by the arrows in pathway A so that the pathway can sustain a metabolic steady flux of M1 to M3. Note that the pathway branches into two subpaths at the position of the enzyme-substrate complex, E1-M2. The upper branch represents diffusional transfer, while the lower branch involves direct transfer. These two branches rejoin at E2-M3 from which the product M3 is obtained. By comparing the fluxes through the two branches at steady state, we determined the relative proportion of reaction that occurs via the two transfer mechanisms.

Three variants of pathway A were also investigated in order to determine if the qualitative properties revealed by our calculations are independent of mechanistic details in the catalytic steps. Pathway B, shown in fig. 4, differs from A in that the catalytic reaction is not allowed in the ternary complex. Pathway C is the same as pathway B with the additional feature that E1 and E2 can combine to form a catalytically inactive complex E1-E2 as in eq. 14. Finally, pathway D, shown in fig. 5, places the branch point at E1-M1 and allows both the E1- and E2-catalyzed reactions to occur within the ternary complexes.

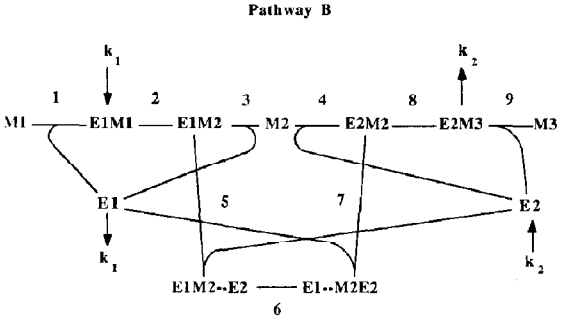

Fig. 4. The hypothetical two-enzyme pathway B.

In each of these pathways there are three types of elementary processes: binding, catalytic, and direct transfer. Each process is indicated by lines connecting reactants and products with reactant lines joining at an acute angle. For example, in pathway A steps 1, 3, 4, 6, 9, and 10 are binding processes; steps 2, 5, and 8 are catalytic reactions, and step 7 is the direct transfer reaction. For pathway A, we have indicated forward rate constants for these reactions by a plus and the reverse rate constants by a minus and grouped them in table 3 according to type. Two additional rate constants, k_{in} and k_{out}, correspond to the input term ($k_{in}a_{E1}$) and the output term ($k_{out}a_{E2\text{-}M3}$) indicated by the arrows in fig. 3. The standard values of these parameters are indicated in parentheses in table 3. We also have used a 'modified standard' set, in which the only change is that protein-protein association rate constants and protein-protein dissociation constants are both reduced by a factor of 10. For pathways B–D, we used analogous standard sets of rate constant values, with each type of rate constant having the same value as for pathway A.

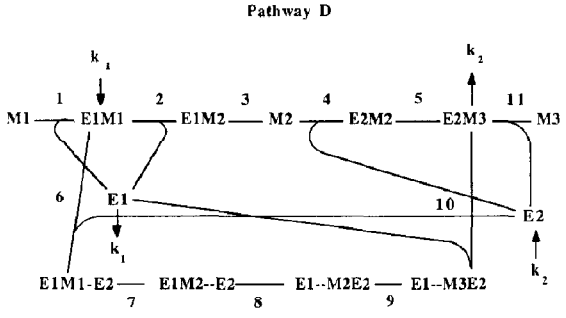

Fig. 5. The hypothetical two-enzyme pathway D.

The standard values were chosen on empirical grounds. 10^8 M^{-1} s^{-1} is well known to be reasonable for the association rate constants of molecules in aqueous solution [30]. For our dehydrogenase simulations we had found that dissociation constants of the order of magnitude of 1 μM for the ternary complexes were required, leading to our choice of 100 s^{-1} for the dissociation rate constants in the case of protein-protein interactions. We also assumed dissociation constants of 1 μM for enzyme-free metabolite interactions, which is the same order of magnitude as that for the dissociation constants of NADH from the dehydrogenases we have studied [9,30]. For direct transfer rate constants, 75 s^{-1} is a value characteristic for the transfer rate constants for NADH between dehydrogenases [10]. Chemical transformations of bound species are generally rapid, for example, the transformation of LDH-bound pyruvate to bound lactate takes place with a rate constant of 1×10^4 s^{-1} [31]; thus, this was chosen as the standard value. Thermodynamics places another restriction on the values of the rate constants. Because the diffusion and direct transfer branches begin and end at the same intermediates (e.g., E1-M1, E2 and E2-M3, E1 for pathway A), the Gibbs free energy change for each branch must be identical. If we sum the free energy changes in each individual step in each branch, as given by eq. 10 applied to each step, and equate the sums, we find that the rate constants must satisfy a cycle identity [32], which for pathway A is

$$(k_{+3}/k_{-3})(k_{+4}/k_{-4})(k_{+5}/k_{-5}) = (k_{+6}/k_{-6})(k_{+7}/k_{-7})(k_{+8}/k_{-8})(k_{+9}/k_{-9}) \quad (17)$$

It is easily verified that both the standard and modified standard values of the rate constants in table 3 satisfy this requirement.

Using these or similar values of the rate constants, integration of pathway A (or its variants) was carried out numerically using PLOD. Starting from initial conditions in which only [E1] and [E2] had nonzero values yielded a steady state for the

Table 3

Rate constants for pathway A [a]

Association rate constants (1×10^8 M^{-1} s^{-1}):
k_{+1}, k_{-3}, k_{+4}, k_{+6}, k_{-9}, k_{-10}
Dissociation rate constants (100 s^{-1}):
k_{-1}, k_{+3}, k_{-4}, k_{-6}, k_{+9}, k_{+10}
Catalytic rate constants (1×10^4 s^{-1}):
k_{+2}, k_{-2}, k_{+5}, k_{-5}, k_{+8}, k_{-8}
Direct transfer rate constants (75 s^{-1}): k_{+7}, k_{-7}
Input and output rate constants (100 s^{-1}): k_{in}, k_{out}

[a] Standard values are in parentheses; the 'modified' standard values are the same except that protein-protein association rate constants are 1×10^7 M^{-1} s^{-1} and the corresponding dissociation rate constants are 10 s^{-1}.

concentrations of all species within 1 s. In the steady state, the fluxes through the steps in the pathway, and the rates of free energy dissipation in those steps, were determined by use of eq. 7 or 8, and eq. 12. When applying eq. 7, it is necessary to switch the sign of the rate if the forward direction of the process in the metabolic pathway is that of association, e.g., for step 10 in pathway A we have

$$R_{10}^{ss} = k_{+10}\gamma_{E2\text{-}M3}[E2\text{-}M3]^{ss} - k_{-10}\gamma_{E2}\gamma_{M3}[E2]^{ss}[M3]^{ss}. \quad (18)$$

where the superscript ss represents steady state. Since there is no accumulation of intermediate species at steady states, it follows that there are then only two independent fluxes, R_{dif}^{ss} for the diffusion branch and R_{dir}^{ss} for the direct transfer branch. Examining pathway A makes clear that the total flux through the pathway is $R_T^{ss} = R_{dif}^{ss} + R_{dir}^{ss}$, which equals the flux through step 1, step 2, or step 10. Similarly, one has $R_3^{ss} = R_4^{ss} = R_5^{ss} = R_{dif}^{ss}$ and $R_6^{ss} = R_7^{ss} = R_8^{ss} = R_9^{ss} = R_{dir}^{ss}$. Comparable results hold for pathways B–D. As a consequence, the fraction of the flux carried by the direct transfer branch is given by R_{dir}^{ss}/R_T^{ss}.

5. Theoretical results

As pointed out in section 4, we were interested in assessing the importance of the direct transfer mechanism under physiological conditions, specifically whether, in a two-enzyme pathway with competing direct transfer and diffusional branches, the flux through the direct transfer branch can be expected to dominate. We examined this issue by varying the concentrations of the enzymes over ranges thought to reflect in vivo conditions and tabulating the fractional flux through the direct transfer branch. We also examined, via this approach, how the fluxes through each branch depend on the concentrations of each enzyme separately, and therefore whether an excess of the first or second enzyme would favor one branch over the other.

Our results are presented in the four ensuing subsections. First, we discuss the dependence of the fractional and total fluxes through pathway A on the concentrations of E1 and E2, assuming activity coefficients of unity, and we examine the dependence of these fluxes on the dissociation constants for the ternary complexes. Then, we determine the effects on these fluxes of increased activity coefficients. Following this we consider to what extent these results are modified for pathways B and D, the effects on the fluxes of introducing the binary E1-E2 complex in pathway C, and the effects of varying the equilibrium constants for the binding of M2 to E1 and E2. In subsection 5.4, we examine the pattern of free energy dissipation without direct transfer and compare it with that obtained when direct transfer operates in pathway B, and the changes in this pattern that occur upon varying particular rate constants or the activity coefficients. We also study here the distribution of metabolites among the various enzyme species and in solution, and changes in this distribution that occur upon varying the rate constants for E1-E2 or ternary complex formation, or the activity coefficients of the enzyme species.

5.1. Kinetics of pathway A

Assuming the standard set of rate constants, we varied total [E1] and [E2] independently over a range of physiologically reasonable values, 10–400 μM, and examined the total flux and the direct transfer and diffusion fluxes. Illustrative results are given in table 4, which presents both the total

flux, in micromoles of metabolite processed by the pathway/liter per second, and the fraction of this flow that passes through the direct transfer branch, as a function of the total concentrations of E1 and E2. The total flux values are not unreasonable physiologically. Consider that a typical value for the rate of glycolysis in exercising skeletal muscle, at a power output that can be sustained for 30 min, might be 2000 mmol kg^{-1} min^{-1} [33]. This corresponds to a flux of approx. 90 μmol l^{-1} s^{-1} through the glycolytic pathway subsequent to aldolase, if the glycolytic enzymes are regarded as evenly distributed throughout muscle tissue. However, these enzymes are restricted to the sarcoplasm, and the volume accessible to them is approximately one-fifth of the entire cellular volume [2], so if we wish to consider the glycolytic flux within a liter of the volume actually accessible to the enzymes, we must multiply the above value by a factor of approx. 5, giving a value similar to those in the table. We found that for [E2] $\geq$ 100 μM the direct transfer flux always dominates strongly. As can be seen by comparing rows 3 and 5, increasing [E1] while keeping [E2] fixed increases the contribution of diffusion (i.e., decreases the fractional flux of direct transfer). As can be observed by comparing rows 2 and 5, increasing [E2] with fixed [E1] increases the contribution of direct transfer. The sudden, strong increase in direct transfer's dominance as [E2] passes [E1], demonstrated by comparing rows 4 and 6 in table 4 is particularly striking. The range of concentrations we have given the enzymes is physiologically realistic, thus our results indicate that direct transfer within transient enzyme complexes in solution may play a dominant role in metabolic pathways, particularly in two-enzyme segments where the concentration of the second enzyme is comparable to that of the first.

Table 4

Total flux and the fraction of flux through direct transfer for pathway A as a function of total enzyme concentrations

[E1] [a] (μM)	[E2] [a] (μM)	Fractional flux through direct transfer branch	Total flux, (μM s^{-1})
100	50	0.55	339
200	50	0.52	342
50	100	0.94	329
100	100	0.77	477
200	100	0.63	501
100	200	0.97	494
100	400	0.99	495

[a] We assumed that μM and μN are the same for these enzymes, i.e., one active site per molecule.

Again using the standard set of rate constants, we varied the dissociation equilibrium constants of the ternary complexes by varying the association and dissociation rate constants for their formation (k_{+6}, k_{-9}, and k_{-6}, k_{+9}; respectively).

Table 5

Total flux and flux through each branch of pathway A as a function of the association and dissociation rate constants for formation of the ternary complexes [a]

k_a	k_d	(E1) (μM)	[E2] (μM)	Fraction of flux through direct transfer	Total flux (μM s^{-1})
10^6	10	200	400	0.45	968
		400	200	0.10	1809
10^8	10	200	400	0.99	210
		400	200	0.53	229
10^6	1000	200	400	0.17	5241
		400	200	0.74	5912
10^8	1000	200	400	0.93	2139
		400	200	0.63	2087
0	-	200	400	0.00	5342
		400	200	0.00	6255

[a] k_a denotes the association rate constant (in either direction) for formation of the ternary complex, in units of μM^{-1} s^{-1}. k_d is the corresponding dissociation rate constant in s^{-1}.

For simplicity, both the association rate constants were assigned the same value k_a, and both the dissociation rate constants were assigned a value k_d. We varied k_a over the range $0–10^9$ M^{-1} s^{-1} and independently varied k_d over the range 1–1000 s^{-1}. Simultaneously, for each of the pairs of k_a and k_d values thereby generated, we allowed total [E1] and total [E2] to assume the values 200 or 400 μM. Illustrative data are presented in table 5. It is evident from comparison of rows 3, 7, and 9 that even with [E1] less than [E2] the total flux increases steadily as the dissociation constant of the complexes ($K_d = k_d/k_a$) is increased, until, with no complex present, it is above its value for the standard parameter set by a factor of approx. 10. The direct transfer flux also increases at first, as can be seen by comparing rows 4 and 8, and there exists a point where the flux through the direct transfer branch is maximized.

We were surprised to find that the diffusional pathway alone processed much more metabolite than the combination of the two (rows 9 and 10), and sought to define conditions that would alter this, considering that the adoption of direct transfer in vivo might be favored under conditions where this dramatic decrease in total flux was not a consequence. This might be the case, for example, if free M2 were unstable to hydrolysis — as, for example, is the glycolytic intermediate 1,3-diphosphoglycerate [8] — which would tend to short-circuit the diffusional transfer process. Therefore, we repeated the series of simulations in table 5 with a rate constant for the first-order disappearance of free M2 by decomposition. We found that the steady increase of the total flux with the dissociation constant of the ternary complexes is still observed unless this rate constant exceeds 15 000 s^{-1}. Thus a free intermediate would have to have an average lifetime of less than 0.1 ms for the introduction of direct transfer to add to the total flux through a segment of a pathway described by our kinetic scheme.

5.2. *Activity effects*

In our investigation of activity effects on the fluxes in pathway A, we were primarily interested in what alterations in the relative contributions of direct and diffusional transfer would be seen as the activity coefficients were increased. The key point here is that the ternary complex is larger than either of the individual enzymes, so its activity coefficient will be larger than that of the individual enzymes if it and the enzymes both 'see' the same surrounding concentration of total protein. To ascertain the quantitative consequences of this effect we assumed the enzymes E1 and E2 to be spheres of equal size and the ternary complex to be a sphere of approximately twice the volume. Thus, we assigned activity coefficients to individual enzymes by considering the individual enzymes to be hard spheres of effective radius 30 Å. Enzyme-enzyme complexes were taken to be spheres of effective radius 40 Å. To generate the activity coefficients, we postulated the existence of 'inert protein' at concentrations typical of total intracellular protein. The activity coefficients of the enzyme species involved in the pathway were generated solely by this inert protein, i.e., the enzyme species did not see each other specifically, rather, they only saw a surrounding milieu of protein at concentrations typical of cellular protein, so that the activity coefficient of each enzyme species did not depend on its own concentration or those of any other enzyme species and was therefore independent of time. Neglecting any effect of bound ligands on activity coefficients, we further assumed that the radii of E1 and E1-M1, for example, were equal, so that their activity coefficients were equal.

Another effect of inert protein, noted by Muramatsu and Minton [39], is the lowering of the diffusion coefficients. This leads to a kind of 'sieving' of reactants, which in the case of diffusion-controlled bimolecular processes will slow their rate [40]. Although there are several bimolecular binding processes in our kinetic schemes, they involve the binding of macromolecules. Macromolecular binding steps tend to have rate constants below the translational diffusion-controlled limit, in part due to their intrinsic rate and in part due to the obligatory angular reorientation that must occur prior to binding [41]. These effects of inert protein are difficult to calculate explicitly and because they are small with respect to activity effects, we have chosen to neglect them here.

We varied the inert protein concentration from 0.17 to 3.57 mM, corresponding to a range of 0.016–0.34 g protein per ml solution if the protein has a specific gravity of 1.4 and an effective radius of 30 Å. A table of activity coefficients obtained in this way is given in the appendix. For each of the inert protein concentrations in our range, we independently varied total [E1] and total [E2] within the range 50–400 μM, with rate constants at their standard values. Illustrative results are given in table 6. It is evident that an increase in protein concentration sharply increases the total flux and the predominance of the direct transfer flux. One expects this a priori because of the high activity coefficients of the ternary complexes (cf. the appendix) that are present in the expressions for the net rates of the elementary processes in the direct transfer branch. It is true that the total flux in these simulations becomes quite high — indeed, above the rate of glycolysis under physiological conditions — but we have verified that the qualitative properties of the flux are unchanged if we lower the input and output rate constants k_{in} and k_{out} to bring the total flux to values similar to those in table 4. In particular, if k_{in} and k_{out} are assigned the same value, the fractional flux through direct transfer is fixed as we vary this value from 5 to 500 s^{-1}, and the total flux is approximately proportional to this value until it exceeds 150 s^{-1}.

The standard set of rate constants yields concentration-based dissociation equilibrium constants of 1 μM for the ternary complexes, which is a rather low value. Therefore, we repeated this set of simulations with the ternary complex association rate constants both set equal to 10^6 M^{-1} s^{-1}, which gives dissociation constants of 100 μM for the ternary complexes, and with all other rate constants at their standard values. Under these conditions, if we set total [E1] = total [E2] = 100 μM, direct transfer accounts for only 15% of the total flux when all activity coefficients are assumed equal to unity. However, when we generated activity coefficients with inert protein with a radius of 30 Å and a concentration of 2.91 mM (corresponding to 260 mg/ml if we assume a specific gravity of 1.3), we found that 63% of the total flux is through the direct transfer branch when total [E1] = total [E2]. This result demonstrates that even very weakly bound ternary complexes can allow direct transfer to predominate if physiologically reasonable concentrations of total protein are present. Furthermore, as long as total [E1] = total [E2], this fractional flux through direct transfer is virtually fixed when total [E1] varies over a range from 25 to 200 μM.

Table 6

Total flux and flux through each branch of pathway A as a function of the concentration of protein present [a]

[Inert protein] (mM)	[E1] (μM)	[E2] (μM)	Fractional flux through direct transfer	Total flux (μM s^{-1})
0	100	100	0.77	477
	100	200	0.97	494
	200	100	0.63	501
0.83	100	100	0.83	745
	100	200	0.98	777
	200	100	0.72	774
2.91	100	100	0.96	4238
	100	200	0.99	4402
	100	400	1.0	4407
	200	100	0.93	4322

[a] Standard values were used for all rate constants.

5.3. *Variations in kinetic mechanism*

We have examined the effect of changing the mechanistic details of pathway A on our results by carrying out similar calculations with pathways B–D. We set parameters at their standard values for these three pathways and varied total [E1] and [E2] over the values 50, 100, 200, and 400 μM, as had been done previously for pathway A. For pathway C, which is identical to pathway B except for the appearance of the noncatalytic complex E1-E2, this series of calculations was carried out with dissociation constants of 10 and 1 μM for the noncatalytic E1-E2 complex. Illustrative data for pathways B–D are given in table 7.

As is evident from comparison of tables 4 and 7, there are only small quantitative differences between pathways A, B, and D in the fraction of the total flux carried by the direct transfer branch.

Table 7

Comparison of fluxes for pathways B, C and D [a]

[E1] (μM)	[E2] (μM)	Fraction of flux through direct transfer	Total flux (μM s^{-1})
Pathway B			
100	100	0.80	571
100	200	0.97	602
200	100	0.68	603
Pathway C, with a dissociation constant of 10 μM for E1-E2			
100	100	0.79	558
100	200	0.97	437
200	100	0.68	601
Pathway C, with a dissociation constant of 1 μM for E1-E2			
100	100	0.77	465
100	200	0.97	95
200	100	0.67	585
Pathway D			
100	100	0.80	419
100	200	0.98	433
200	100	0.68	438

[a] Standard values were used for all rate constants, except that for formation of noncatalytic E1-E2 complex the association rate constant was 10^7 M^{-1} s^{-1} and the dissociation rate constant was either 100 or 10 s^{-1}.

Specifically, the flux through direct transfer for given total [E1] and [E2] is enhanced 15–30% in pathway B and diminished 20–30% in pathway D, with respect to pathway A. The diffusional and total fluxes are also enhanced in pathway B and diminished in pathway D, by virtually the same percentages. Examination of the steady-state concentrations revealed that increasing the number of intermediate species in the direct-transfer branch diminishes the concentration of each one, and also that the concentrations of free E1 and E2, which are needed to combine with intermediate species, are reduced. This effect is sufficient to account for diminished fluxes in both pathways. Although not shown here, these calculations were repeated to assess the effect of inert protein, which was assumed to be present in the concentration range 0.166–3.57 mM. Again, only the same minor quantitative differences were observed. Since pathways A, B, and D differ only in whether catalysis takes place in one, both, or neither of the enzymes in the ternary complex, we conclude that our results obtained in subsections 5.1 and 5.2 concerning the qualitative properties of the fractional and total fluxes are independent of the mechanistic details of the direct transfer step. The concentrations of the various species and the fluxes through the steps of the pathway are determined by eqs 7 and 8, and these quantities are related to the rates of dissipation of free energy within the steps through eq. 12. Thus it follows that since the differences in fluxes and concentrations among pathways A, B, and D are minor, so are the differences in rates of free energy dissipation in the steps they share in common.

The calculations for pathway C reveal that noncatalytic E1-E2 complexation diminishes the flux through both branches by approximately equal percentages. The total flux is lowered by a much greater amount if E2 is in excess than if E1 is in excess, as is particularly evident from comparison of rows 8 and 9 of table 7. In fact, when the species concentrations at steady state were examined, we found that under the conditions corresponding to row 8 of table 7 the concentration of E1-E2 was 94 μM, whereas under the conditions corresponding to row 9 this value was reduced to 5.2 μM.

We further examined whether the inhibitory effect of noncatalytic E1-E2 complexation would be moderated under physiological conditions by the existence of a pathway for direct transfer. We varied the dissociation rate constant for E1-E2 over the range 0.2–2000 s^{-1}, while the association rate constant was varied independently over the range 2×10^5–2×10^9 M^{-1} s^{-1}. For these calculations we set total E1 and E2 concentrations at 100 μM, used an inert protein concentration of 2.32 mM to generate activity coefficients, and assumed modified standard values for rate constants. These calculations were carried out with and without ternary complex formation, so that we were able to compare the inhibitory effect of E1-E2 with direct transfer operative to that without direct transfer operative. We also repeated this series of simulations with M2 more tightly bound to E1 and E2, with both dissociation constants 0.1 μM.

It was found in all cases that the steady-state fluxes only depend on the E1-E2 dissociation equi-

librium constant k_d/k_a, not on the individual magnitudes of the rate constants. This is expected since the elementary process of E1-E2 formation comes to equilibrium at steady state, i.e., zero flux occurs through this step, so one may apply eqs 10–11b with $\Delta G = 0$, obtaining ([E1][E2])/([E1-E2]) = (k_d/k_a). The presence of direct transfer greatly decreases the effect on the flux of catalytically inactive E1-E2 complexation. For example, with dissociation constants for M2 of 1 μM, the total flux through pathway C only decreases to 80% of its original value (with no E1-E2 complex) when E1-E2 complex is allowed to form with a dissociation constant of 1 μM. Almost all of this decrease is in the flux through the direct transfer branch. However, when the direct transfer branch is not operative, the total flux decreases by a factor of 5. It was also found that tighter binding of free M2 strongly decreases the efficacy of diffusional transfer. When both binding dissociation constants are decreased from 1 to 0.1 μM, the flux through the diffusion pathway operating alone decreases by approximately a factor of 5, becoming less than the total flux found when direct transfer is operative with all rate constants at modified standard values. In the latter case, the decrease in the total flux upon the same alteration of dissociation constants is in fact negligible — less than 5%. This conclusion holds whether or not catalytically inactive complex is allowed to form. Thus it appears that tight binding of free intermediate is a much stronger factor than instability of free intermediate in determining when the adoption of direct transfer functions to increase the total flux through a pathway.

5.4. *Species concentrations and energy dissipation*

We chose pathway B for examination of these matters because it is the simplest of the four pathways and, as noted previously, we expect the results to generalize qualitatively to pathways A and D. In studying the concentration dependencies, we focused on three issues of physiological importance. Firstly, we looked at the manner in which varying amounts of inert protein would affect the concentrations and the distribution of intermediate metabolite between bound vs free forms. Then we examined how these quantities were affected by 'switching on' direct transfer through decreasing the dissociation equilibrium constants of the ternary complexes, and finally we investigated how these quantities were affected by introducing noncatalytic complex as in pathway C and varying the value of its dissociation constant.

To assess the effect of inert protein, we varied the concentration of inert protein over the range 0.166–3.57 mM and examined the steady-state concentrations of all species in pathway B. Other conditions were that all rate constants had standard values and total [E1] = [E2] = 100 μM. We found that as the activity coefficients rose, there was a progressive increase in the concentration of the ternary complexes, which have the highest activity coefficient, and a progressive decrease in the concentration of all other enzyme species of 25–35% from the lowest to the highest inert protein concentration. This is not surprising given that the fractional flux through direct transfer increases steadily as seen before (table 6). The concentrations of free M1 and M3 rose slightly as that of inert protein rose from 0.166 to 3.57 mM, while free M2 did not change.

To assess the effect of nonproductive E1-E2 complexation, we varied the dissociation constant for this complex over the range 1–200 μM with all other rate constants at standard values and with total [E1] = [E2] = 100 μM. In agreement with our earlier finding that both the direct transfer and diffusional flux decrease but that the fractional flux through direct transfer also decreases as this dissociation constant was lowered, we found that the concentrations of the ternary complexes decreased much more rapidly than those of the enzyme species in the diffusion branch. We found only a small increase in the concentration of free metabolites as [E1-E2] increases. When the dissociation constant for E1-E2 is 1 μM, its concentration is 29 μM, approximately the same as that of each ternary complex.

To assess the effect of varying the rate constants for ternary complex formation, we set both association rate constants equal to a single parameter k_a, and the dissociation rate constants equal to a single parameter k_d, and varied k_a over the range of $0–10^7$ M^{-1} s^{-1} while keeping k_d fixed at

10 s^{-1}. This corresponds to 'turning on' direct transfer from an initial state without ternary complex by lowering the dissociation equilibrium constant of the ternary complex. The concentrations of all species as a function of this dissociation constant are illustrated in fig. 6. The changes seen upon lowering the dissociation constant by alteration of one rate constant are as one would expect — the concentration of ternary complex increases, leaving less free enzyme and binary enzyme-substrate complexes, so that the concentration of free M1 and M3 increases slightly in turn. However, the total M1 and M3 concentrations decrease considerably because of the decrease in binary enzyme-substrate complexes, with the percentage change in total M1 or M3 much higher than that for free M1 or M3. The total M2 concentration also increases considerably. Thus we have increases in the percentage of bound M2 and the percentages of free M1 and M3. This and the other methods of altering species concentrations that we have examined are potential modes of regulation that may be applied in particular metabolic pathways to change the concentrations of several species in a coherent fashion, including species removed by one or more steps from the reaction where the regulation is applied.

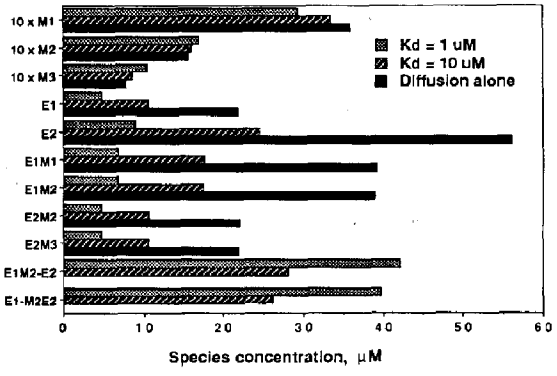

Fig. 6. The steady-state concentrations of the species in pathway B as a function of the dissociation constants of the ternary complexes, both of which are set equal to a parameter K_d, the value of which is varied over 1, 10, and 100 μM. The case of diffusion operating alone is also illustrated. To vary K_d, both dissociation rate constants were held at 10 s^{-1} and both association rate constants were varied over the values 10^7, 10^6, and 10^5 M^{-1} s^{-1}. All other rate constants were at standard values and the total concentrations of E1 and E2 were each 100 μM. Note that the concentrations of M1, M2, and M3 have been multiplied by 10.

The free energy dissipation rate at a given step in a metabolic pathway is defined as the flux through that step multiplied by the change in free energy at that step (eq. 12). Dissipation rates provide a quantitative measure of where the unavoidable 'chemical friction' in the pathway creates losses of chemical energy [19]. The steps of pathway B are numbered 1–9 as indicated in fig. 4. As an example of the application of eq. 12, if we denote the activity coefficient for individual enzyme by γ_1 and the activity coefficient for ternary complex by γ_2, the free energy dissipation rate for Step 5 is given by

$$\Phi_5 = R_5 \Delta G_5$$

with

$$R_5 = \left(k_{+5}\gamma_1^2[\text{E1-M2}][\text{E2}] - k_{-5}\gamma_2[\text{E1M2-E2}]\right) \tag{19}$$

and

$$\Delta G_5 = \left\{ RT \ln\frac{k_{+5}}{k_{-5}} + RT \ln\left(\frac{\gamma_2[\text{E1M2-E2}]}{\gamma_1^2[\text{E2}][\text{E1-M2}]}\right)\right\}$$

The separate expressions for the rate and for the change in free energy are obtained from eq. 6 by taking 'E' = E1-M2, 'S' = E2, and 'E-S' = E1M2-E2; and via eqs 10–11b. Note that since steps 1 and 9 are considered completely irreversible, neither a ΔG nor a Φ can be defined for them.

We first looked at the dependence of the rates of free energy dissipation in the various steps as a function of the concentration of inert protein. Using modified standard values for all rate constants and setting total [E1] = [E2] = 100 μM, we varied the activity coefficients by varying the concentration of inert protein over the range 0.17–3.57 mM. As before, inert protein was considered as solely generating the activity coefficients. The magnitudes of dissipation obtained are illustrated in table 8; note that the absolute value of each Φ is tabulated. The largest dissipation rates, together accounting for 40–75% of the total, are found in the two steps (nos 5 and 8) of ternary complex formation in the direct transfer branch, and the

percentage of total free energy dissipation occurring in these steps increases steadily with the concentration of inert protein. As the activity coefficients increase dissipation rates in the diffusion branch actually drop for both steps, while dissipation rates in each direct transfer and catalytic step increase steadily, the increases of highest percentage occurring in the catalytic steps. It is also evident that the free energy differences across all steps except the catalytic steps 2 and 8 decrease as the concentration of inert protein increases, implying that the other steps approach equilibrium.

This can be understood in the following way. The forward and reverse rates of elementary processes in the direct transfer branch involve either the activity coefficient of the ternary complexes or the square of the activity coefficient for the individual enzymes. Therefore, these forward and reverse rates become large much more rapidly than all the other rates in the pathway, in particular, more rapidly than the input and output rate terms $k_{in}\gamma_{E1}[E1]$ and $k_{out}\gamma_{E2M3}[E2M3]$. Thus the concentrations of species in the direct transfer branch must approach their equilibrium values, giving rise to very large forward and reverse rates that nearly cancel and yield the smaller net flux through this branch. As the direct transfer branch comes to equilibrium, so must the diffusion branch, since the branches have common endpoints. However, the free energy difference across the catalytic steps increases with the activity coefficients, because the flux is determined by a rate expression proportional to only the first power of the activity coefficient. Thus the concentrations of the species in this step must remain well out of equilibrium to maintain this total flux.

The catalytic steps dissipate little energy, particularly when the activity coefficients are low. These steps are close to equilibrium because of their large rate constants, so that lowering the catalytic rate constants increased these dissipation rates. For example, if both forward catalytic rate constants are given values of 100 s^{-1}, and both reverse rate constants values of 10 s^{-1}, 82% of the total energy dissipated arises from the catalytic steps 2 and 8. Although there was a significant increase merely because the rate constants were slowed down, a more important quantity is the equilibrium constant for the catalytic step. Whenever this quantity is increased the catalytic dissipation increases markedly. The same behavior was observed when the direct transfer branch was not operative, and we have carried out calculations that show similar behavior occurring in other steps of the pathway.

Table 8

The magnitudes of free energy changes and dissipation rates in the steps of pathway B as functions of inert protein concentration [a]

Concentration of inert protein (mM)	Dissipation rate per step and $\lvert\Delta G\rvert$ per step								Total flux and % through direct transfer
		Diffusion		Direct transfer					
	2	3	4	5	6	7	8	Total	
0.17	0.21	9.4	8.2	4.4	0.54	7.3	0.33	30.5	506
	(4.1)	(314)	(274)	(210)	(34)	(340)	(5.9)	(596)	(40)
1.99	0.91	10.5	9.6	17.3	2.0	23.4	0.97	64.7	1811
	(4.8)	(180)	(165)	(141)	(21)	(183)	(5.9)	(356)	(67)
2.91	4.1	6.3	6.0	37.0	4.0	42.4	3.9	104	4765
	(5.3)	(96)	(91)	(82)	(12)	(93)	(5.9)	(198)	(83)
3.57	6.4	4.2	4.1	45.0	4.7	48.6	7.0	120	11712
	(5.6)	(46)	(45)	(41)	(5.7)	(45)	(5.8)	(102)	(92)

[a] Total [E1] = [E2] = 100 μM, all rate constants are at modified standard values. ΔGs and flux percentages through direct transfer are given in parentheses. Units of ΔG are cal mol^{-1}, those of the dissipation rates are (cal l^{-1} s^{-1})×100, and those of total flux are μM s^{-1}. The total ΔG is for the overall reaction, E1M1 + E2 = E1 + E2M3.

We also examined the manner in which the pattern of free energy dissipation and the ΔG values changed as the dissociation equilibrium constant of the ternary complex was decreased from infinity to 1 μM, in exactly the same way as that used to generate fig. 6. The results are listed in table 9. Generally a smooth transfer of dissipation from the diffusional branch to the direct transfer branch is observed as the dissociation constant of the ternary complexes decreases. The rates of dissipation in the catalytic steps parallel the total dissipation rate in decreasing with the dissociation constant of the ternary complexes, as is expected because of the decrease in the total flux. It is evident that disassembly of the ternary complex into free M2 + E1 + E2 is always an energetically favorable process, i.e., the ΔG for reversal of step 5 followed by execution of step 3 is always negative by 0.1–0.22 kcal/mol. Thus, as direct transfer is turned on, M2 bound in ternary complex, with a higher free-energy content per mole than free M2, is created — i.e., if M2 was to be used in another metabolic process, the ternary complex could first be disassembled, yielding extra free energy (this is a small effect, however, compared to other ΔG values of reaction in glycolysis, which can be many kilocalories [3]). In order to examine further the effects of the adoption of direct transfer on the storage and utilization of free energy in metabolism, one would naturally have to know the mechanisms by which M2 was actually processed in other reactions. Nonetheless, with direct transfer operating the intermediate M2 does reside in a state of higher free energy in the ternary complex than free in solution.

6. Discussion

We have seen that the putative evidence from kinetic experiments for direct transfer of NADH among dehydrogenases, particularly between α-GDH and LDH, can be reproduced by our numerical simulations, but only if strong enzyme-enzyme interactions, resulting in dissociation constants for ternary complexes of the order of 1 μM, are assumed. In order to fit experimental data, we have had to assume in addition that such interactions operate for both the formation of ternary complexes E1-NADH-E2 and of noncatalytic complexes E1-E2*, where the asterisk indicates that E2 is bound by a second substrate. Dissociation constants in this range, in fact, are comparable with estimates of K_m values for the reduction of E1-NADH by E2 [9] for dehydrogenases. We emphasize that the nature of the ternary complexes that appear in our work is dynamic, i.e., their association and dissociation rate constants are both significant, so that individual complexes

Table 9

The magnitudes of free energy changes and dissipation rates in the steps of pathway B as functions of the association and dissociation rate constants of the ternary complexes [a]

Rate constants		Dissipation rate per step and $\lvert\Delta G\rvert$ per step							
k_a	k_d		Diffusion		Direct transfer				
		2	3	4	5	6	7	8	Total
0	0	0.73	106	89.2	–	–	–	1.3	198
		(3.3)	(487)	(408)	(–)	(–)	(–)	(5.9)	(904)
10^5	10	0.61	84.4	71.1	1.5	0.19	3.0	1.1	162
		(3.4)	(480)	(400)	(266)	(47)	(563)	(5.9)	(890)
10^6	10	0.38	39.4	33.4	3.9	0.51	7.7	0.61	85.9
		(3.5)	(431)	(365)	(252)	(43)	(500)	(5.9)	(803)
10^7	10	0.19	9.2	8.0	4.0	0.49	6.7	0.32	28.8
		(4.0)	(322)	(281)	(211)	(35)	(358)	(5.9)	(614)

[a] Total [E1] = [E2] = 100 μM; all rate constants are at modified standard values. Units and notation are as in table 8.

exist for less than 100 ms or so. Thus it would be impossible to separate these complexes from individual molecules of E1 or E2 by such methods as analytical ultracentrifugation or gel filtration, for example.

However, our calculations show that for direct transfer to be significant in both steady-state and transient experiments, a large fraction of the enzymes must be found in ternary complexes. Our calculations suggest that noncatalytic E1-E2* complex formation may occur even in the absence of NADH. One method to detect such complexes is to label one enzyme with a fluorescent probe whose spectrum is very sensitive to the environment and look for a spectral change as the other enzyme is titrated, as described in ref. 34. Another, more decisive, technique is light scattering, either classical [35] or quasi-elastic [36], either of which is well established as a method for determination of molecular sizes in solution. Still another technique is sedimentation equilibrium centrifugation, the theoretical description of which has recently been extended to nonideal, concentrated macromolecular solutions by use of scaled-particle theory [37,38]. Our calculations imply that if direct transfer is functioning as a significant metabolite transfer mechanism, then sufficient concentrations of ternary complex will be formed under accessible laboratory conditions to detect the complexes by these methods. The A-B dehydrogenases, carefully titrated with NADH, seem like an ideal system for such experiments.

The existing evidence for direct transfer is largely circumstantial and, in some cases, controversial. In order to establish unequivocally that direct transfer exists, it is essential to verify the existence of ternary complexes by direct physicochemical means. If a signal for ternary complex formation, such as a change in the spectrum of a fluorescent probe, can be found, one might then determine the association and dissociation rate constants for complex formation by monitoring of this signal in a stopped-flow kinetic experiment. If ternary complexes can be observed, it would also be important to determine whether the enhancement of the rate constants for transfer of NADH between dehydrogenases within a ternary complex that we have been forced to invoke here (from 32 to 700 s^{-1}) does, in fact, occur when the second substrate for one of the dehydrogenases is present. The stopped-flow experiments that have been used to estimate values for these rate constants in the absence of the second substrate [4,12] should also be repeated in the presence of a nonreactive analog of the second substrate (a competitive inhibitor), such as oxamate for LDH.

The central result from our simulations of hypothetical enzyme pathways is that if direct transfer exists, it can provide a significant mechanism for the processing of metabolite in vivo. This was found using the criteria of the fractional flux carried by the direct transfer branch and the energy dissipation, both under physiologically reasonable enzyme concentrations, activities, kinetic mechanisms, and values of the rate constants for the elementary processes involved. The presence of inert protein at a moderate concentration greatly increases the importance of direct transfer, to the point where a dissociation constant of 100 μM for the ternary complexes is sufficient to make direct transfer dominant over diffusional transfer. This increases the probability that direct transfer plays an important role physiologically and suggests that in vitro the addition of inert polymer should significantly increase effects attributable to channeling of metabolite through complexes, such as a reduction in the transient time required for the production of final product to reach its steady-state rate [13] or a reduction in the proportion of metabolite diverted by a competing enzymatic reaction the substrate of which is an intermediate metabolite free in solution. We have seen, furthermore, that our qualitative results remain unchanged when we consider variant pathways in which catalysis is or is not allowed to take place in the ternary complexes.

We have examined conditions under which adoption of the direct transfer mechanism might increase the total flux, since in some situations, such as glycolysis in muscle tissue, it would appear to be advantageous to adopt mechanisms that would maximize the flux through the pathway at times of stress. It is evident that the flux through the diffusion pathway operating alone is often considerably greater than that obtained when direct transfer is operating in parallel. The phenom-

enon of nonproductive protein aggregation, which may be quite important under the conditions of high protein concentration in the cell, tends to eliminate this advantage. Instability of the free intermediate M2 in solution, which could be due to chemical decomposition or consumption by a competing enzymatic reaction, is not a strong effector of the flux through the diffusion pathway operating alone or in parallel with direct transfer. The strength of binding of M2 to E1 and E2 is much more effective. There are other cases in which it would not be to the advantage of an organism to increase the total flux, which might need instead to be kept within a narrow range. Then the adoption of direct transfer may provide new opportunities for regulation, for example, by alteration of the dissociation equilibrium constants of the ternary complexes [9]. In addition to regulation of fluxes, there could be regulation of the concentrations of the various enzymatic species and free metabolites by such alterations, as well as by alterations of other rate constants in the pathway. We are currently examining how effectors of such enzymatic interactions could help regulate glycolysis.

Finally, we have examined the consequences of direct transfer for the thermodynamics of intermediary metabolites by calculating steady-state concentrations, free energy differences, and dissipation rates for individual steps in our hypothetical reaction pathways. By systematically increasing the importance of direct transfer by decreasing the rate constant for dissociation of the ternary complexes, we have found significant effects of direct transfer on the thermodynamics of the pathway. In particular, the free-energy content of the ternary complex exceeds that of free M2, so that for these species free energy is preferentially stored in the direct transfer branch. Also, under standard conditions we have found that the majority of free energy dissipation occurs in the steps of ternary complex formation; however, dissipation by the catalytic steps can dominate if small catalytic rate constants are assumed. We hope that experimental characterization of the extent to which direct transfer actually functions in glycolysis soon will allow the significance of these thermodynamic and kinetic effects to be ascertained.

Appendix

To calculate the activity coefficient of the i-th spherical species, γ_i, in a solution composed of m species of hard spheres, we applied the following result of scaled-particle theory [26]

$$\ln \gamma_i = -\ln(1-S_3) + \left[\frac{6S_2}{1-S_3}\right] r_i + \left[\frac{12S_1}{1-S_3} + \frac{18S_2^2}{(1-S_3)^2}\right] r_i^2 + \left[\frac{8S_0}{1-S_3} + \frac{24S_1S_2}{(1-S_3)^2} + \frac{24S_2^3}{(1-S_3)^3}\right] r_i^3 \tag{A1}$$

where r_i is the effective radius of the i-th species and S_j is determined by ρ_i, the number density of the i-th species, according to

$$S_j = \frac{\pi}{6} \sum_{i=1}^{m} \rho_i (2r_i)^j.$$

As an example of the activity coefficients generated under plausible physiological conditions, assume we have in solution enzymes E1 and E2, each spherical with effective radius 30 Å, and also have E1-E2 complex, regarded as spherical with effective radius 40 Å. Suppose inert protein, spherical with effective radius 30 Å, is present and is solely responsible for generating activity coefficients for the enzymes and complex. That is, in the expression for S_j above one only sums over one term, which contains the number density and effective radius of inert protein. Then the following activity coefficients are obtained as a function of the inert protein concentration.

[Inert protein] (mM)	Activity coefficient of E1 or E2	Activity coefficient of the ternary complex
0.17	1.10	1.16
0.83	1.66	2.26
1.99	4.23	10.8
2.57	7.76	30.9
2.91	11.6	62.5
3.57	30.0	342

Acknowledgements

This work was supported in part by the Agricultural Experiment Station of the University of California and in part by NSF Grant CHE 86-18647. We gratefully acknowledge programming assistance provided by John Wagner and fruitful conversations with D.K. Srivastava. This work was inspired by an incipient collaboration with Sidney Bernhard, which was cut short by his death. We dedicate this paper to his memory.

References

1 P. Srere, Ann. Rev. Biochem. 56 (1987) 89.
2 D. Srivastava and S. Bernhard, Curr. Top. Cell. Regul. 28 (1986) 1.
3 A. Lehninger, Biochemistry (Worth, New York, 1975).
4 D. Srivastava and S. Bernhard, Annu. Rev. Biophys. Biophys. Chem. 16 (1987) 175.
5 J. Clegg, Am. J. Physiol. 246, (1984) R133.
6 P. Friedrich, Supramolecular enzyme organization (Pergamon, Oxford, 1984).
7 G. Welch, Prog. Biophys. Mol. Biol. 32 (1977) 103.
8 J. Weber and S. Bernhard, Biochemistry 21 (1982) 4189.
9 D. Srivastava and S. Bernhard, Biochemistry 24 (1985) 623.
10 D. Srivastava and S. Bernhard, Biochemistry 26 (1987) 1240.
11 D. Srivastava and S. Bernhard, Science 234 (1986) 1081.
12 D. Srivastava, P. Smolen, G. Betts, T. Fukushima, H. Spivey and S. Bernhard, Proc. Natl. Acad. Sci. U.S.A. 86 (1989) 6464.
13 T. Keleti, B. Vertessey and G. Welch, J. Theor. Biol. 135 (1988) 75.
14 J. Kvassman and G. Pettersson, Eur. J. Biochem. 186 (1989) 261.
15 J. Kvassman and G. Pettersson, Eur. J. Biochem. 186 (1989) 265.
16 J. Kvassman, G. Pettersson and U. Ryde-Pettersson, Eur. J. Biochem. 172, (1987) 427.
17 D. Srivastava, S. Bernhard, R. Langridge and J. McClarin, Biochemistry 24 (1985) 629.
18 B. Chock and H. Gutfreund, Proc. Natl. Acad. Sci. U.S.A. 85 (1988) 8870.
19 J. Keizer, Statistical thermodynamics of nonequilibrium processes (Springer, New York, 1987).
20 A. Minton, Biopolymers 20 (1981) 2093.
21 D. Kahaner and D. Barnett (1988) PLOD, version 4.9, National Institute of Science and Technology, Washington, DC.
22 A. Hindmarsh, Ordinary differential equation solver, Report UCID-30001 (1974), Lawrence Livermore Laboratory.
23 G. Castellan, Physical chemistry (Addison-Wesley, Reading, MS, 1983).
24 D. Fitts, Nonequilibrium thermodynamics (McGraw-Hill, New York, 1962).
25 A. Minton and P. Ross, Mol. Cell. Biochem. 55 (1983) 119.
26 P. Ross and A. Minton, Biochem. Biophys. Res. Commun. 88 (1979) 1308.
27 A. Minton and H. Edelhoch, Biopolymers 21 (1982) 451.
28 P. Ross and A. Minton, J. Mol. Biol. 112 (1977) 437.
29 A. Minton and J. Wilf, Biochemistry 20 (1981) 4821.
30 A. Fersht, Enzyme structure and mechanism (Freeman, San Francisco, 1977).
31 M. Hardman, J. Coates and H. Gutfreund, Biochem. J. 171 (1978) 215.
32 T. Hill, Free energy transduction in biology (Wiley, New York, 1977).
33 E. Hultman and R. Harris, in: Principles of exercise biochemistry, ed. J. Poortmans (S. Kargel, Basel, 1988) p. 78.
34 F. Wu, L. Yarbrough and C. Wu, Biochemistry 15 (1976) 3254.
35 H. Elias, Macromolecules, I; Structure and properties (Plenum, New York, 1984).
36 J. Earnshaw and M. Steer, The application of laser light scattering to the study of biological motion (Plenum, New York, 1983).
37 R. Chatelier and A. Minton, Biopolymers 26 (1987) 507.
38 R. Chatelier and A. Minton, Biopolymers 26 (1987) 1097.
39 N. Muramatsu and A. Minton, Proc. Natl. Acad. Sci. USA 85, 2984 (1988).
40 J. Keizer, Chem. Rev. 87 (1987) 167.
41 D. Shoup, G. Lipari and A. Szabo, Biophys. J. 36 (1981) 697.